

# Large Format 15 $\mu$ m Pitch XBn Detector

Yoram Karni<sup>\*</sup>, Eran Avnon, Michael Ben Ezra<sup>†</sup>, Eyal Berkowicz, Omer Cohen, Yossef Cohen, Roman Dobromislin, Itay Hirsh, Olga Klin, Philip Klipstein, Inna Lukomsky, Michal Nitzani, Igor Pivnik, Omer Rozenberg, Itay Shtrichman, Michael Singer, Shay Sulimani, Avi Tuito<sup>†</sup>, Eliezer Weiss

SemiConductor Devices P.O. Box 2250, Haifa 31021, Israel

<sup>†</sup> Israel MOD

## ABSTRACT

Over the past few years, a new type of High Operating Temperature (HOT) photon detector has been developed at SCD, which operates in the blue part of the MWIR atmospheric window (3.4 - 4.2  $\mu$ m). This window is generally more transparent than the red part of the MWIR window (4.4 - 4.9  $\mu$ m), and thus is especially useful for mid and long range applications. The detector has an InAsSb active layer and is based on the new "XBn" device concept, which eliminates Generation-Recombination dark current and enables operation at temperatures of 150K or higher, while maintaining excellent image quality. Such high operating temperatures reduce the cooling requirements of Focal Plane Array (FPA) detectors dramatically, and allow the use of a smaller closed-cycle Stirling cooler. As a result, the complete Integrated Detector Cooler Assembly (IDCA) has about 60% lower power consumption and a much longer lifetime compared with IDCAs based on standard InSb detectors and coolers operating at 77K.

In this work we present a new large format IDCA designed for 150K operation. The 15  $\mu$ m pitch 1280 $\times$ 1024 FPA is based on SCD's XBn technology and digital Hercules ROIC. The FPA is housed in a robust Dewar and is integrated with Ricor's K508N Stirling cryo-cooler. The IDCA has a weight of  $\sim$ 750 gram and its power consumption is  $\sim$  5.5 W at a frame rate of 100Hz. The Mean Time to Failure (MTTF) of the IDCA is more than 20,000 hours, greatly facilitating 24/7 operation.

We describe key electro-optical performance parameters of the new detector.

**Keywords:** Infrared Detector, Focal Plane Array, Bariode, InAsSb, XBn, nBn, High Operating Temperature, ROIC, Detector Dewar Cooler, MTF, IDCA

\* Corresponding author

## 1. Introduction

Current trends in the development of infrared (IR) detector arrays are to increase the number of pixels, to reduce their size and to increase the operational temperature of the focal plane array. These serve the combined purpose of increasing the spatial resolution and field of view (FOV) of the image, and reducing the detector power consumption and maintenance costs. They also allow a reduction in the overall system size, by maintaining a similar resolution but with smaller and lighter optics (shorter focal length and smaller optical diameter). In previous papers we presented SCD's mega-pixel InSb detector, Hercules, which has a 1280×1024 array format and a 15μm pitch,<sup>1, 2</sup> and Kinglet, a very low Size, Weight and Power (SWaP) 640×512 15μm pitch integrated detector cooler assembly (IDCA) based on our novel XBn technology<sup>3</sup>. In this paper we present Hercules XBn, which combines the large format with the XBn technology.

High-end Focal Plane Array (FPA) detectors used for imaging in the MWIR wavelength range are traditionally made from Mercury Cadmium Telluride (MCT) or Indium Antimonide (InSb). The best MCT photodiodes are grown on Cadmium Zinc Telluride (CZT) substrates and are Diffusion dark current limited. The dominant contribution to the dark current comes from thermal generation of electron-hole pairs in the photon absorbing layer, followed by diffusion of the minority carriers to the depletion region<sup>4</sup>. This current typically varies as  $T^3 \exp(-\frac{E_g^0}{k_B T})$  where  $E_g^0$  is the bandgap

extrapolated to zero temperature, T is the temperature and  $k_B$  is Boltzman's constant. However CZT substrates are hard to produce, especially in large dimensions, making scaling of the detector to large areas with many pixels very expensive. In contrast, InSb FPAs are easier to produce in large areas and with a high uniformity, because they are manufactured from high quality InSb wafers available with diameters of up to 5".

The dark current in an InSb photodiode typically varies as  $T^{3/2} \exp(-\frac{E_g^0}{2k_B T})$  because it is dominated by the generation of electrons and holes by Shockley - Read - Hall (SRH) traps. These are located in the depletion region of the device, with energies near the center of the bandgap<sup>5</sup>. This "Generation – Recombination (G-R)" dark current is larger than the Diffusion dark current, so an InSb FPA needs to be operated at around 80K in order to achieve low enough dark current for high quality image.

Currently, SCD is one of the largest manufacturers in the world of InSb FPAs. These FPAs are based on two technologies. The first is a planar process utilizing an n-type InSb wafer implanted with a Beryllium junction. These FPAs are traditionally operated at ~77 K - 80K. The second technology uses an epitaxial p-n structure grown by Molecular Beam Epitaxy (MBE). The grown wafer is etched into mesa based pixels and then passivated. Because the quality of the MBE grown junction is higher than that of an implanted junction, the number of SRH traps is lower and these detectors operate with the same performance as the planar technology, but at a higher temperature of 95-100K. The temperature dependence of the dark current is depicted schematically on an Arrhenius plot in Figure1 for the two technologies: by a solid grey curve for planar InSb and by a dotted grey curve for Epi-InSb. The latter lies below the former because it contains a reduced concentration of SRH traps. The grey arrow pointing to the left shows how the operating temperature at a given dark current increases on going from planar to Epi-InSb.

It was proposed by Klipstein that a Bariode or XBn detector<sup>6</sup> that uses InAsSb sensing material grown on GaSb will have diffusion limited dark current like MCT but with the benefit of III-V group materials like InSb. A bipolar design ( $C_p B_n n$ ) was proposed by Klipstein in 2003<sup>7</sup>. A unipolar  $nB_n n$  version was proposed in 2006<sup>8</sup>. Last year we have reported the beginning of production of Hot PelicanD, a 640×512 15μm FPA representing our first product based on XBn technology. In this paper we report on the completion of development of Hercules XBn, a 1280×1024 (1.3 Mpixel) 15μm pitch, array. The rapid and successful development of this large format detector is another proof of maturity of the new technology.

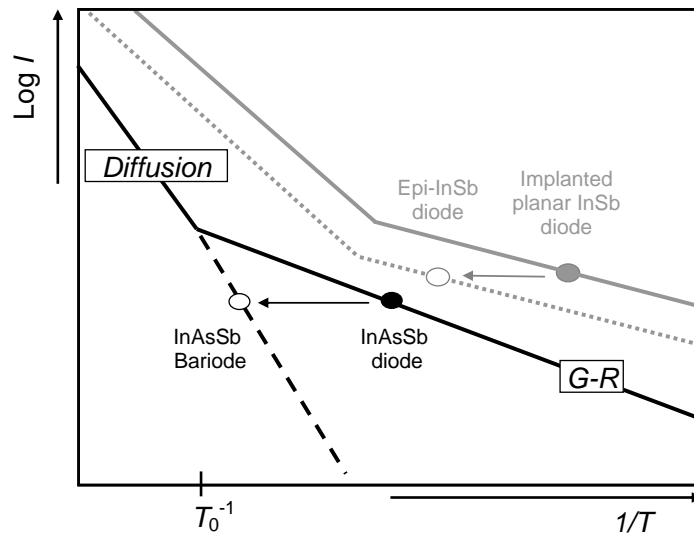


Figure 1 Schematic Arrhenius plot of temperature dependence of the dark current in InSb diodes in which the p-n junction is made by ion-implantation or grown by MBE (Grey), and InAs<sub>0.91</sub>Sb<sub>0.09</sub> diodes and bariodes grown by MBE (Black). The diffusion and G-R limited portions of the InAs<sub>0.91</sub>Sb<sub>0.09</sub> curves are labeled.

Large format arrays are especially important for situational awareness applications, where information is collected continuously and there is a benefit to registering information from a large field of view. In this type of mission, the IDCA is sometimes operated 24 hours a day and 7 days a week, thereby accumulating many operational hours. The mean time to failure (MTTF) of the IDCA becomes a major factor in the cost and operability of these systems. In InSb based IDCAs, failure of the closed loop Stirling cooler is the most frequent cause of failure. This is mainly related to mechanical wear of the cooler's bearing due to its continuous work under high pressure for long periods. Our XBn technology working at 4.2 μm is typically operated at 150K, so cooling down and maintaining the FPA at this temperature requires much less work from the compressor inside the cooler. The compressor works under lower pressure and wear over a given period of time is reduced dramatically. The maximal theoretical cooling efficiency of a Carnot cycle operating between hot and cold thermal reservoirs at temperatures  $T_h$  and  $T_c$ , respectively, is  $\eta_c = T_c / (T_h - T_c)$ . When operated at 27C the maximal theoretical efficiency for maintaining an FPA at 150 K is 1. At 120K the Carnot efficiency is 0.66 and at 77K it falls to 0.35. The actual efficiency of all cryogenic coolers is always lower than the theoretical Carnot value, due to losses in the compressor and to non-ideal thermal properties of selected materials. Raising the FPA temperature to 150K also reduces the conductive thermal load by ~33% compared with an FPA temperature of 77K. Cooler manufacturers optimize the compressor and other cooler parts to have optimal efficiency according to the mission profile, and until recently this was mainly cooling to 77-120K. It is foreseen that when cooler efficiency will be optimized for 150K even lower cooling power will be needed

In the case of the Hercules XBn, which uses the Ricor K508N cooler, the cooler is expected to reach an MTTF of 26000 hours and the IDCA, an MTTF of 20000 hours. The cooler power consumption at 27C is 5.5 Watt, which should be compared with an InSb based Hercules IDCA cooled by a K548 cooler to 80K, which consumes 15W.

## 2. Hercules XBn IDCA

The Hercules XBn IDCA is depicted in Figure 2. The detector is designed for a large FOV and high resolution, so it has a cold shield with an F/number of 2. It is based on a 15μm pitch 1280x1024 XBn-InAsSb array bonded to an extended version of SCD's Hercules digital CMOS ROIC. The Dewar has support ring that serve to damp vibrations in the cold finger and to minimize lateral movement of the FPA. Yet this detector is cooled by the relatively small RICOR K508N Stirling cycle cooler. The Dewar has been optimized to ensure a long vacuum life.

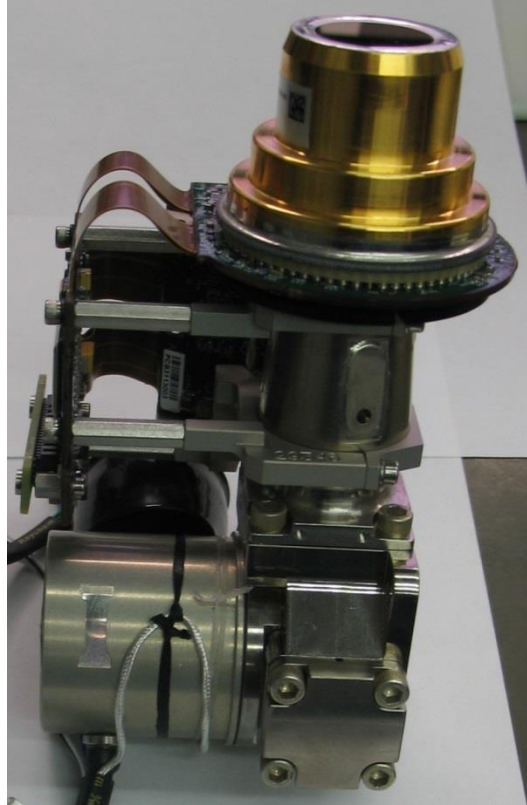


Figure 2 Hercules XBn IDCA

The cooler power consumption is 5.5W at room temperature. At 60% well fill of its 6 Me<sup>-</sup> capacitor, the Hercules XBn detector offers a Noise Equivalent Temperature Difference (NETD, defined in the next section) of < 25 mK. For 60% well fill of its 1 Me<sup>-</sup> capacitor, the NETD is below 35 mK, and with F/2 optics this can be achieved at a maximum frame rate of 100Hz. However, the detector NETD is not necessarily the most critical factor when it comes to mid- or long-range imaging<sup>5</sup>, where other factors, such as atmospheric transmission become important. The overall performance of the Hercules XBn detector is summarized in Table I.

### 3. Electro-optical performance

In this section we describe some of the typical electro-optical performance results of the Hercules XBn detector. Figure 3 shows a typical raw image from a detector operating at 150 K, when placed in front of a black body heated to 53°C. Black and white dots indicate defective pixels. This detector has a total of 1110 defective pixels (0.08%) that are defined as defective according to criteria described in Table 1. The signal drops towards the corners due to the standard cos<sup>4</sup> $\theta$  intensity distribution of the cold shield. Figure 4 depicts an image registered after a two point correction. It demonstrates the high image quality, even on the highly expanded scale used in this Figure.

The performance of an array detector is determined by several key properties. First, the sensitivity is normally defined by the ratio of the temporal noise to the responsivity, and is known as the Noise Equivalent Temperature Difference (NETD). Second, the spatial noise is defined by the Residual Non Uniformity (RNU) following a non-uniformity correction (NUC) procedure. Third, the spatial resolution, which is limited by inter-pixel cross-talk (XT) is best described by the Modulation Transfer Function (MTF). In this section we present an evaluation of these properties in the Hercules XBn FPA, which are related both to the XBn detector and to the ReadOut Integrated Circuit (ROIC).

<b>Parameter</b>	<b>Hercules XBn</b>
Format & pitch	1280x1024, 15 $\mu\text{m}$
Well fill capacity	6 Me <sup>-</sup> & 1 Me <sup>-</sup>
Digital signal resolution	Up to 15 bit
Integration modes	ITR, IWR, Combined
Maximum Frame rate (13bit)	100 Hz @ 1280x1024
FPA power consumption	170 mW @100 Hz
NETD	< 25 mK (@ 60% w.f. 6Me <sup>-</sup> )
RNU	< 0.03 % of the dynamic range
Operability	>99.5%
Power consumption at 23°C (inc. proximity electronics)	5.5W @ 100Hz
FPA temperature	150 K
Readout noise	230e <sup>-</sup> & 850e <sup>-</sup>
Spectral band  (IDCA – cold filter dependent)	3.4- 4.2 $\mu\text{m}$
Cooler	Ricor K508N
MTTF	20,000 hr
Cold Shield height & F#,	28.15 mm, F/2

**Table 1 Overall performance parameters of the Hercules XBn detector**

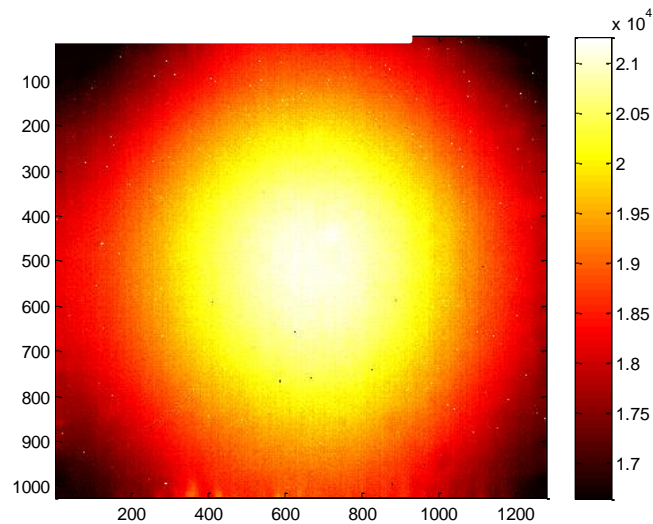


Figure 3 Raw Signal in front of a uniform target at 50% Well Fill. The non-uniformity is due to the familiar  $\cos^4\theta$  effect. No bad pixel replacement was done. The FPA temperature is 150K. The signal measured in digital levels (DL).

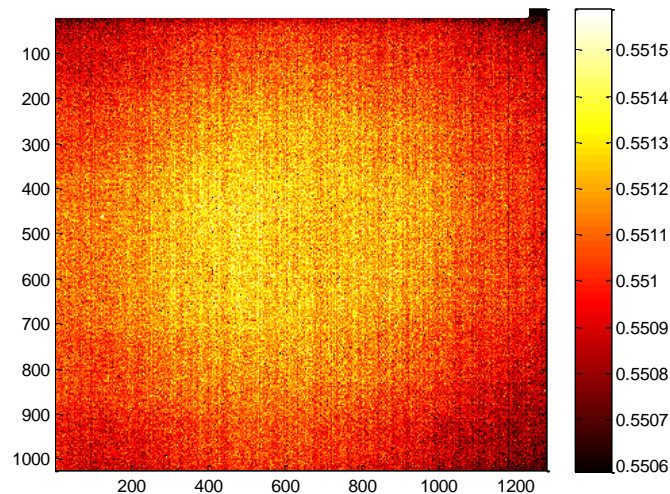


Figure 4 Two-point corrected of a uniform target at 53°C (Well Fill scale)

A critical FPA quality parameter is the number of defective pixels in the FPA and by their distribution. A minimum standard requires that 99.5% of the pixels should be operational. Normally, with InSb arrays, this standard is easily achieved. The situation with XBN technology is similar, as shown in Figure 5, where we present a defective pixels map for a typical FPA. This FPA has 1110 defective pixels that are only 0.08% of the 1.3 Mpixels on the detector, and are distributed uniformly over the array area with no large clusters, making the entire array area usable. Some large format arrays tend to suffer from disconnected corner pixels. This, however, is not the case with the Hercules XBN FPA, as can be seen by the almost empty field in the disconnections map depicted in Figure 6 .

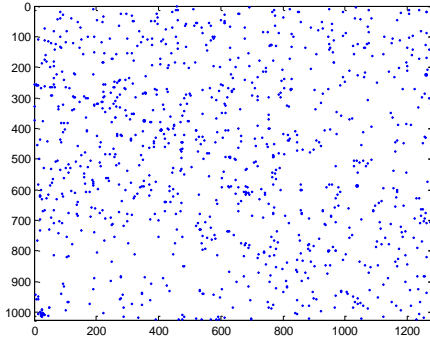


Figure 5 Defective Pixel map – total of 1110 defects out of 1.3Mpixels (0.08%) at 150K

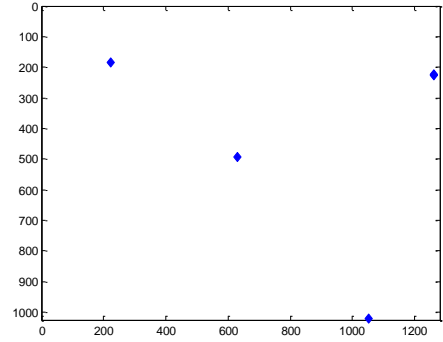


Figure 6 Disconnected pixels Map showing 5 disconnected pixels

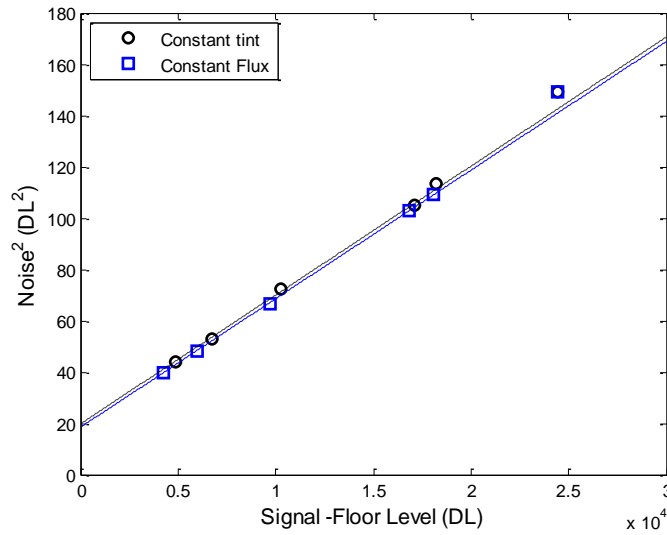


Figure7 Noise Squared as a function of signal in XBN FPA showing a gain of 180 e/DL and readout noise of 789 e<sup>-</sup> for the 6 Me<sup>-</sup> capacitor.

Figure7 shows the square of the noise measured as function of the signal. It can be shown that the slope of this curve is equal to the reciprocal of the ROIC gain, and the interpolation to zero integration time gives the detector readout noise. In this detector, these values are 188 e-/Digital Level (DL) for the gain and 789e- for the readout noise. The linearity of this curve also indicates shot-noise behaviour of the signal without any additional source of noise, such as 1/f noise.

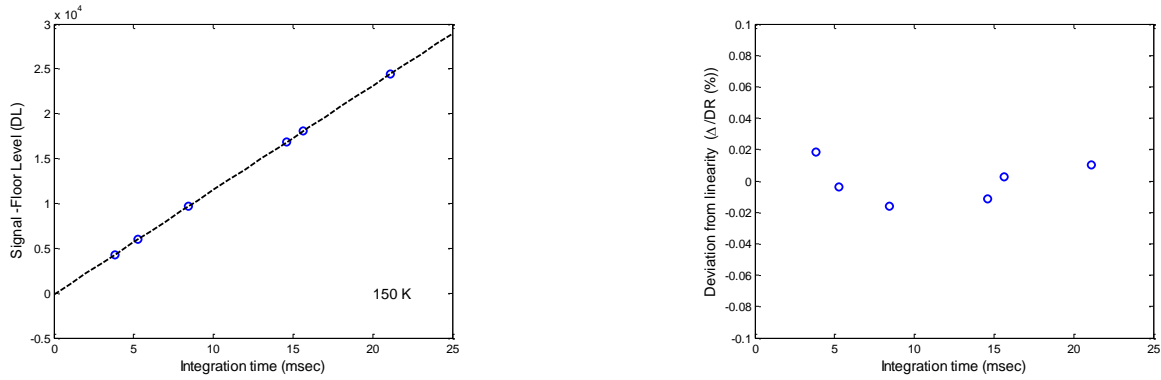


Figure 8 a. Signal vs integration time and b. signal deviation from linearity

Figure 8 demonstrates the excellent linearity of the ROIC over almost the entire dynamic range (DR) of the detector. The uniformity of the III-V XBn pixels after a 2-point linear NUC is very good as well, due also to the linearity and high dynamic resistance of the pixels. In order to calculate the correction coefficients, the detector is placed in front of a uniform extended black-body and measurements are recorded at two different black-body temperatures, keeping the integration time constant. The signal is averaged over a sequence of 32 consecutive frames in order to reduce the effect of the temporal noise on the spatial correction. The two measured signals are at approximately 20% and 80% well-fill. Using these measurements, the correction coefficients are calculated and used to correct the signal at other black-body temperatures, while keeping the same integration time. The quality of the correction is determined by the spatial standard deviation (STD) of all non-defective pixels of the FPA after the correction, when placed in front of a uniform target. This spatial STD, also known as the RNU of the detector, is plotted as a function of well-fill in Figure 9. As can be seen in the Figure, the RNU is less than 0.02% of the DR over a wide range of well-fills. At the correction points, the STD is zero by definition. Due to the raw signal non-uniformity caused by the cold shield shadowing of a uniform target ( $\cos^4\theta$  effect), the maximal well-fill at the edge is around 85% when the first central pixel is saturated.

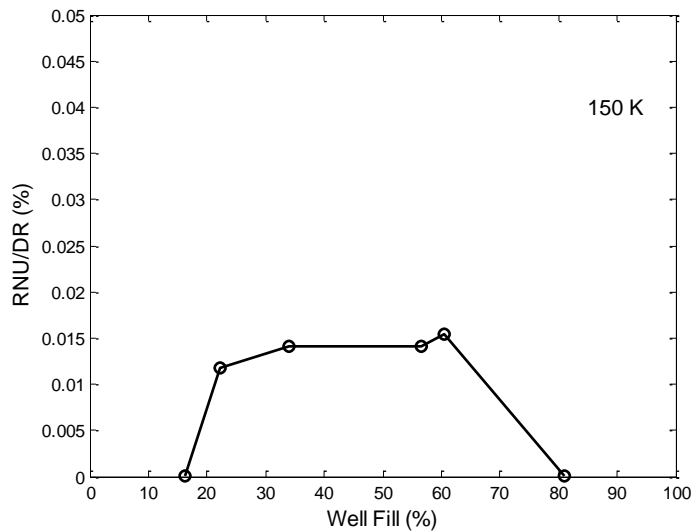
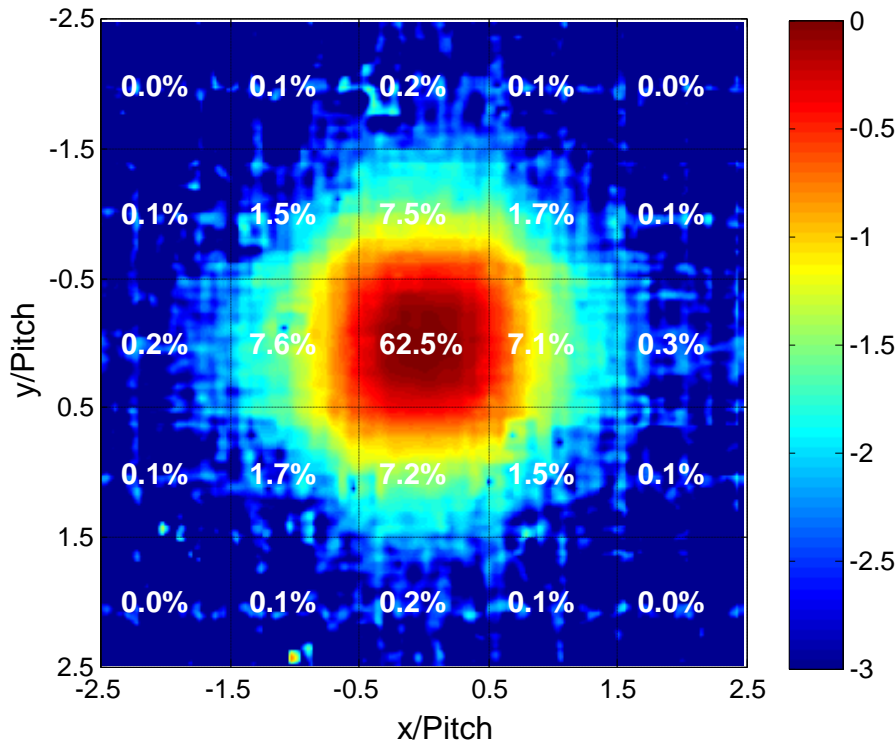


Figure 9 RNU as function of Well Fill. The integration time was held constant and the flux was varied



Ideally, the spatial resolution of the FPA itself (not including diffraction effects due to system optics) is determined by the pixel size. However, in a real detector, the pixels are coupled by optical and electrical mechanisms, known as pixel crosstalk (XT), which can smear the image. When one pixel in the FPA is illuminated at its center by a "delta function" source, the response will not only be in that pixel but also in neighboring pixels. In order to measure the crosstalk, the detector was illuminated by a  $4 \times 4 \mu\text{m}^2$  spot that was scanned over the array. As neighboring pixels were illuminated, the photo current was measured only on the central pixel. Figure 10 depicts the crosstalk map that is deduced from this "point spread function" measurement. Because the XBn structure is grown by MBE, the active layer thickness can be controlled precisely and is not affected by procedures such as substrate removal. Due to the thin active layer, the nearest neighbor crosstalk is rather low, at the level of only 7%.



**Figure 10** Two dimensional point spread function and crosstalk values in  $15\mu\text{m}$  pitch XBn FPA at 150 K. The central pixel is illuminated with a  $4 \times 4 \mu\text{m}^2$  spot and the signal measured each pixel is normalized to the sum of measured signal through a five by five array. The color scale is logarithmic

The spectral response at 150K of the  $15\mu\text{m}$  pixels pitch XBn FPA was described in Ref. 3 The typical cut-off wavelength (at 50% of the initial rise) is  $\sim 4.2 \mu\text{m}$  and that the Quantum Efficiency (QE) is above 70% for wavelengths shorter than  $4.1 \mu\text{m}$ . The spectral response is fairly flat over most of the blue MWIR, SWIR and NIR windows to  $1 \mu\text{m}$ , with values in the 80- 85% range.

XBn detectors have very low dark current due to the elimination of GR contribution. Figure 11 shows the logarithm of the dark current, averaged over all non-defective pixels in the FPA, as a function of the reciprocal temperature, for two different detectors. In each case, the results exhibit a near linear dependence over the range of 120-260K and fit the expression  $T^3 \exp(-E_g^0/k_B T)$  very well with a value of  $E_g^0$  close to the bandgap of the photon absorbing layer. This is the expected behaviour for Diffusion current, and is a good indication that the GR current

has been entirely eliminated. Figure 12 depicts a histogram of the dark current at 150K. It shows a narrow bell curve distribution, with a peak at 0.38 pA and a width of 25fA.

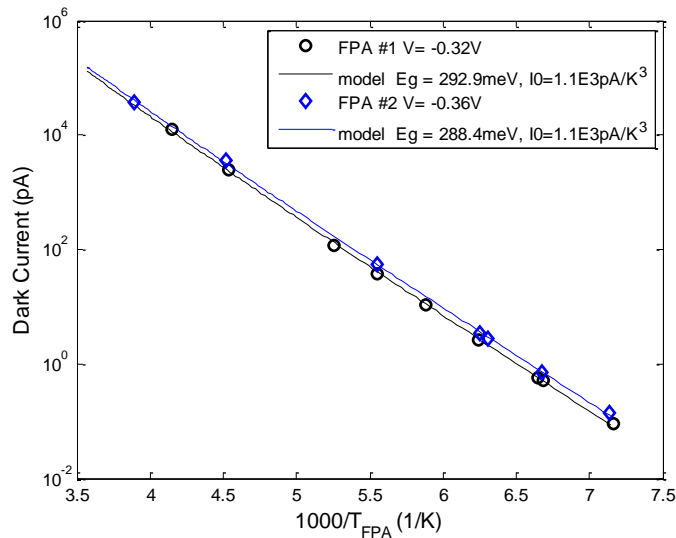


Figure 11 Average dark current in XBn FPA vs. inverse temp. The solid lines are fit to the model

$$I_d = I_0 \exp\left(-\frac{E_g}{k_B T}\right)$$

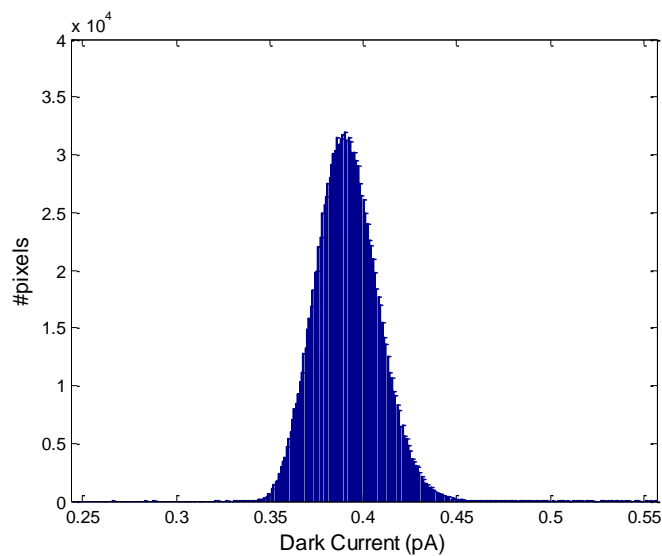


Figure 12 Typical Dark current histogram at 150K

#### **4. Conclusions**

We have presented a new HOT detector in of SCD's product line, based on XBN technology. Similar to the PelicanD detector presented last year, the HOT Hercules 1280×1024 array detector with a 15 μm pixel has a very low dark current at a high operating temperature of 150K. The Hercules detector, with its excellent performance, low power consumption and high reliability, is well suited for missions where it must be operated 24 hours a day, 7 days a week.

The new HOT Hercules detector is based on a new, extended version of SCD's Hercules digital ROIC. The Hercules ROIC has been optimized for use with XBN devices, and has a very low read-out noise. Its bias range has been extended and the capacitor sizes have been optimized for a detector with a 4.2 μm cut-off wavelength.

## 5. References

- [1] Shkedy, L., Markovitz, T., Calahorra, Z., Hirsh, I. and Shtrichman, I. "Megapixel digital InSb detector for midwave infrared imaging", *Optical Engineering* 50 (6), June 2011.
- [2] Neshet, O., Pivnik, I., Ilan, E., Calahorra, Z., Koifman, A., Vaserman, I., Oiknie Schlesinger, J., Gazit R., and Hirsh, I., "High resolution 1280×1024, 15  $\mu\text{m}$  pitch compact InSb IR detector with on-chip ADC", *Proceedings of SPIE*, Vol. 7298, *Infrared Technology and Applications XXXV Conference* (2009), pp 72983K-1-9.
- [3] Klipstein, P.C., Gross, Y., Aronov, D., Ben Ezra, M., Berkowicz, E., Cohen, Y., Fraenkel, R., Glozman, A., Grossman, S., Klin, O., Lukomsky, I., Markowitz, T., Shkedy, L., Shtrichman, I., Snapi, N., Tuito, A., Yassen, M., and Weiss E., " Low SWaP MWIR detector based on XBn Focal Plane Array" *Proceedings of SPIE*, Vol. 8704, *Infrared Technology and Applications XXXV Conference* (2012)
- [4] Tennant, W.E., "Rule 07 revisited: still a good heuristic predictor for p/n HgCdTe photodiode performance?" *J. Electron. Mater.* 39, 1030, (2010)
- [5] Klipstein, P.C., Klin, O., Grossman, S., Snapi, N., Lukomsky, I., Yassen, M., Aronov, D., Berkowicz, E., Glozman, A., Fishman, T., Magen, O., Shtrichman, I. and Weiss, E., "XBn barrier Photodetectors based on InAsSb with high operating temperatures", *J. Opt. Engineering* **50**, 061002, (2011)
- [6] Klipstein, P.C., "XBn Barrier Photodetectors for High Sensitivity and High Operating Temperature Infrared Sensors", *Proc. SPIE* 6940, 6940-2U, (2008)
- [7] Klipstein, P.C. "Depletionless Photodiode with Suppressed Dark Current...", US Patent 7,795,640 (2 July 2003)
- [8] Klipstein, P.C., Unipolar semiconductor photodetector with Suppressed Dark Current..., US Patent 8,004,012 (6 April 2006)
- [9] Klipstein, P.C., Aronov, D., Berkowicz, E., Fraenkel, R., Glozman, A., Grossman, S., Klin, O., Lukomsky, I., Shtrichman, I., Snapi, N., Yassen, M., and Weiss E., "New "bariodes" device reduces cooling requirements of infrared detectors", *SPIE Newsroom* 10.1117/2.120110.00319 (November 2011)